



HAL
open science

Phantomas: a flexible software library to simulate diffusion MR phantoms

Emmanuel Caruyer, Alessandro Daducci, Maxime Descoteaux,
Jean-Christophe Houde, Jean-Philippe Thiran, Ragini Verma

► **To cite this version:**

Emmanuel Caruyer, Alessandro Daducci, Maxime Descoteaux, Jean-Christophe Houde, Jean-Philippe Thiran, et al.. Phantomas: a flexible software library to simulate diffusion MR phantoms. ISMRM, May 2014, Milan, Italy. hal-00944644

HAL Id: hal-00944644

<https://inria.hal.science/hal-00944644v1>

Submitted on 10 Feb 2014

HAL is a multi-disciplinary open access archive for the deposit and dissemination of scientific research documents, whether they are published or not. The documents may come from teaching and research institutions in France or abroad, or from public or private research centers.

L'archive ouverte pluridisciplinaire **HAL**, est destinée au dépôt et à la diffusion de documents scientifiques de niveau recherche, publiés ou non, émanant des établissements d'enseignement et de recherche français ou étrangers, des laboratoires publics ou privés.

Phantoms: a flexible software library to simulate diffusion MR phantoms

Emmanuel Caruyer¹, Alessandro Daducci², Maxime Descoteaux³, Jean-Christophe Houde³, Jean-Philippe Thiran², and Ragini Verma¹

¹Section of Biomedical Image Analysis, Department of Radiology, University of Pennsylvania, Philadelphia, PA, United States, ²Signal Processing Laboratory 5, École Polytechnique Fédérale de Lausanne, Lausanne, Vaud, Switzerland, ³Sherbrooke Connectivity Imaging Lab, Université de Sherbrooke, Sherbrooke, Québec, Canada

Target audience— We introduce *Phantomas*, an open-source software library to create realistic phantoms in structural and diffusion MRI. This is intended as a tool for researchers working in method development or translational research in the field of diffusion-weighted MRI. The software allows evaluation of the whole tractography processing pipeline: acquisition design, preprocessing, local reconstruction and tractography algorithm.

Purpose— Diffusion MRI has been an active area of research for the last two decades. However, while the data processing pipeline from DWIs to fiber tracking involves several steps, it is still difficult to evaluate the influence of a specific noise reduction method, a specific representation of the angular diffusion information, or a specific tracking algorithm, on fiber tracking results. By starting from a ground truth configuration of fiber bundle geometries, *Phantomas* is designed to enable quantitative assessment of each step involved in the pipeline, using metrics based on successful reconstruction of the true connectivity profile of the phantom, such as defined in *Tractometer*¹. Complementarily, for the evaluation of local reconstruction accuracy, local metrics² can be computed to measure the accuracy of angular models. Existing softwares^{8,9} present similar objectives, yet *Phantomas* offers an original perspective in the computation of volume fraction (VF), signal attenuation and T1/T2 images.

Methods— *Geometric primitives*. The phantom mimics a portion of the brain, with white matter fiber bundles connecting different cortical regions. Each fiber bundle is represented by a tube of constant radius wrapped around its centerline. The centerlines are defined as 3rd-order piecewise polynomials, controlled by user-defined control points. The centerlines are further constrained to be normal to the surface, which represents the gray-white matter interface. An example of a fiber configuration is represented in Fig. 1a. We also introduce some water-filled regions, represented as spheres, and a shell of water-filled material surrounding the phantom, intended to mimic the cerebrospinal fluid around the brain tissue.

Tissue volume fraction. In order to simulate MR signal on a grid of given resolution, the first step is to identify the VF of each tissue type: white matter (WM), gray matter (GM) and cerebrospinal fluid (CSF). This is done in a hierarchical fashion: first, for each geometric primitive, we identify a map of voxels intersected by the corresponding object. Then for each voxel either partially filled by an object, or intersected by many objects, we evaluate the VF on a grid subdivision of the given voxel. This two-step procedure allows for an efficient computation of the VF for the whole dataset.

Signal relaxation. The influence of longitudinal and transverse relaxation on the signal decay is also considered. Relaxation times reported in vivo⁶ vary across individuals and across brain regions. We simulate maps of T1 and T2 relaxation times of the same resolution as the target image, using Gaussian distributed samples with the following mean and standard deviations (in ms): GM T1=1331±13, T2=110±2; WM T1=832±10, T2=79.6±0.6; CSF T1=3500±100, T2=250±10. A correlation ratio of 0.2 is introduced between direct neighboring voxels, which are not statistically independent. The image correlation matrix is factorized using Cholesky decomposition to simulate random image; since the dimension of the problem is large, but the covariance matrix is sparse, efficient algorithms³ are used to solve the factorization problem.

Fiber orientation distribution and signal attenuation. As for the simulation of tissue VF, the estimation of the fiber orientation distribution (FOD) in a given voxel starts by the computation of fiber orientation samples, corresponding to the closest orientation of each bundle on a regular subdivision of the voxel. Then, we use kernel density estimation with a symmetric Von-Mises Fischer kernel to estimate a continuous FOD. The signal attenuation in WM is computed based on a composite hindered and restricted model of diffusion⁴, where the extra-axonal compartment is modeled by a diffusion tensor and the intra-axonal compartment is modeled by a cylinder⁷. Since this model has cylindrical symmetry, the attenuation is computed as the convolution of the FOD with a template diffusion profile. This is done to save computational complexity, since the computation of the cylindrical restricted compartment is time and resource consuming.

Results— We simulated a configuration of 27 fiber bundles, on a 70x70x70 grid, with 3 spherical regions of free water, represented in Fig. 1.a. The range of fiber configurations includes fiber bending, crossings, and kissing fibers. As a result, a range of intravoxel white matter configurations were created, with a total of 3695 voxels in pure WM, out of which 1192 contain more than one (and up to 5) fiber bundles. Besides, 15482 voxels contain a fraction of WM, and a fraction of GM and/or CSF. Crossing angles range from 0 to 90°, as reported in Fig. 1.c. The simulation of 64 volumes of DWIs ($b = 3000\text{s/mm}^2$) were completed in about 15 minutes on a standard laptop. An example of fiber reconstruction using MRtrix⁵ probabilistic tracking on constrained spherical deconvolution is reported in Fig. 1.d.

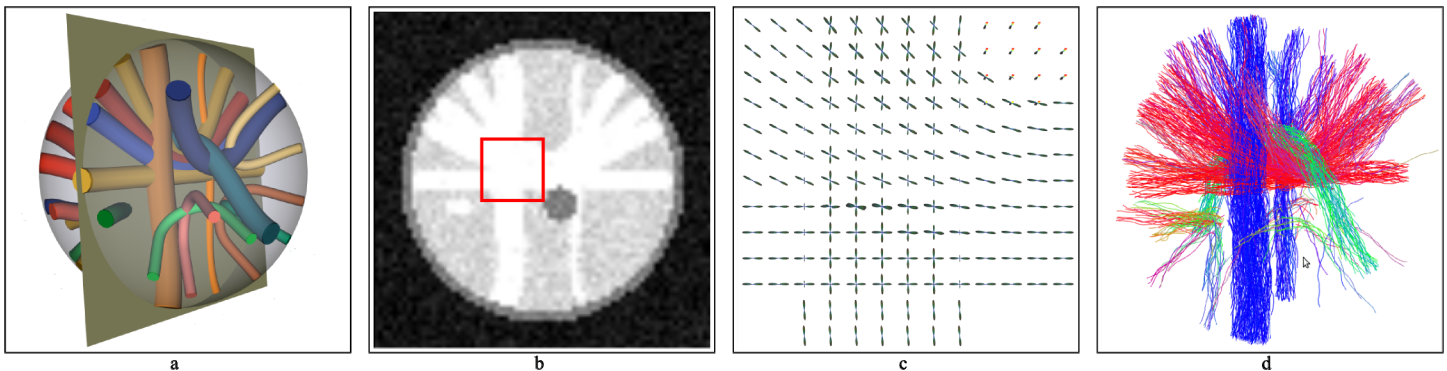


Figure 1. a. An example of fiber bundle configuration, and spherical regions filled with free water. b. Corresponding slice of T1-weighted image. c. Ground truth fiber orientation distribution (zoom of the red square in 1.b). d. Fiber reconstructed with probabilistic streamline tracking using MRtrix⁵.

Conclusions— We believe that *Phantomas* will have a positive impact on the community for the validation and the development of novel methods in diffusion MRI. An early version of this tool was used successfully to create the testing dataset of the 2nd HARDI Reconstruction Challenge, organized at ISBI, San Francisco, CA, USA (2013). The software is released as a free and open-source software library written in Python and ANSI C, and is designed towards flexible use and integration with other software.

References— 1. M.-A. Côté et al., *MedIA*, 17(3), pp. 844-857, 2013. 2. A. Daducci et al., *TMI*, in press. 3. T. A. Davis and W. W. Hager, *ACM Trans. Math. Software*, 35, 2009. 4. Y. Assaf et al., *Neuroimage* 27(1), pp. 48-58, 2005. 5. J. Tournier et al., *Int J Imag Syst Tech* 22(1), pp. 53-66, 2012. 6. J. P. Wansapura et al., *JMRI* 9(4), pp. 531-538, 1999. 7. O. Söderman and B. Jönsson, *JMR*, A 117(1), pp. 94-97, 1995. 8. P. F. Neher et al., *ISMRM*, 20013. 9. T. G. Close et al., *NeuroImage*, 47(4), pp. 1288-1300, 2009.